Thin Solid Films 627 (2017) 39–43

Contents lists available at ScienceDirect

Thin Solid Films

journal homepage: www.elsevier.com/locate/tsf

Low-temperature growth of graphene on iron substrate by molecular beam epitaxy

Renjing Zheng [a], Zhongguang Xu [a], Alireza Khanaki [a], Hao Tian [a], Zheng Zuo [a], Jian-Guo Zheng [b], Jianlin Liu [a,*]

[a] Quantum Structures Laboratory, Department of Electrical and Computer Engineering, University of California, Riverside, CA 92521, USA
[b] Irvine Materials Research Institute, University of California, Irvine, CA 92697, USA

ARTICLE INFO

Article history:
Received 10 August 2016
Received in revised form 9 December 2016
Accepted 25 February 2017
Available online 27 February 2017

Keywords:
Graphene
Fe
Molecular beam epitaxy
Low temperature growth

ABSTRACT

Graphene has attracted a great deal of interest due to its fascinating properties and a wide variety of potential applications. Several methods have been used to achieve high-quality graphene films on different substrates. However, there have been only a few studies on graphene growth on iron (Fe) and the growth mechanism remains unclear. This paper systematically investigates temperature-dependent growth of graphene on Fe substrate by gas-source molecular beam epitaxy. Two-dimensional (2D), large-area graphene samples were grown on Fe thin films, and characterized by Raman, X-ray photoelectron spectroscopy, X-ray diffraction, optical microscopy, transmission electron microscopy and atomic force microscopy. It is found that graphene flakes can be grown on Fe at a growth temperature as low as 400 °C and the optimized large-area graphene growth temperature is relatively low between 500 °C and 550 °C. The graphene growth on Fe that undergoes the formation and decomposition of iron carbide is discussed.

1. Introduction

Graphene is composed of single-layer or few-layer sp^2-bonded carbon (C) atoms arranged in a two-dimensional hexagonal crystal lattice, and its lateral dimension can span from nanoscale to wafer-scale. Numerous researchers have looked into methods for producing highly crystalline wafer-scale graphene because of its outstanding properties and a wide variety of potential applications. These methods include "scotch tape" approach for exfoliating graphene from highly ordered pyrolytic graphite (HOPG) [1], graphitization of silicon carbide surfaces [2–4], and epitaxial growth on catalytic metal substrates using chemical vapor deposition (CVD) [5–7] and molecular beam epitaxy (MBE) [8,9]. Among these methods, the epitaxial growth can produce large-size graphene layers in a controllable manner. To date, various transition metals have been used as templates or substrates for high-quality graphene synthesis [5–12]. Compared with other metals, such as Ni, Co, Pt, there are very few reports about graphene growth on iron (Fe) [13–15], which is the most widespread transition metal. The main reason could be the challenging procedure of graphene growth on Fe due to its higher chemical reactivity compared with other transition metals. In addition, its growth mechanism, which may correlate with the complex Fe-C phases, remains elusive.

In this paper, we demonstrate low-temperature growth of high-quality, large-area graphene thin films on Fe substrates by gas-source MBE. Various characterization methods have been employed to assess the films. Unique mechanism involving the formation/decomposition of iron carbide (Fe_xC_y) is responsible for the growth of graphene on Fe, in contrast to precipitation of C atoms without involving metal carbides from other metals. The formation of graphene by involving the chemical reaction between Fe and C rather than temperature-sensitive physical precipitation process enables precise control of the thickness of the film because the reaction of Fe and C can be well controlled at certain temperature, compared with drastic wide-range temperature change requirement for the precipitation growth of graphene on other metals. Moreover, the reaction of Fe and C can occur at relatively low temperature, leading to low-temperature synthesis of graphene. Thus, this work not only elucidates the mechanism of graphene growth on Fe but also provides a convenient route to achieve scalable epitaxial graphene films for those applications that can only sustain moderate- and low-temperature processes.

2. Materials and methods

2.1. Growth method

A Perkin-Elmer MBE system was used for graphene growth. Acetylene gas (C_2H_2, Airgas, 99.9999%) was connected to the MBE chamber as a C source and the flow rate was tuned by a mass flow controller (MFC). H_2 gas (Airgas, 99.9999%) was also introduced to the chamber by a needle valve during the process when necessary. An Fe film of

* Corresponding author.
E-mail address: jianlin@ece.ucr.edu (J. Liu).

http://dx.doi.org/10.1016/j.tsf.2017.02.057
0040-6090/

300 nm was grown on a SiO_2/Si wafer by an e-beam evaporator and used as substrate. After the substrate was transferred to the growth chamber, the substrate was heated to a targeted growth temperature between 250 °C and 800 °C at a rate of 10 °C/min and annealed for 10 min. During the annealing process, 10 sccm H_2 was introduced into the chamber to remove possible iron oxide and suppress evaporation of Fe. After that, H_2 flow rate was decreased to 6 sccm, and the graphene growth started by the introduction of 5 sccm acetylene. During the growth, the pressure was usually between ~1×10^{-4} and 1×10^{-5} Torr depending on the source flow rates. The growth lasted for 2 min. After the growth, the sample was slowly cooled to room temperature at a rate of 10 °C/min.

2.2. Characterization methods

Optical microscopy and Raman characterization were performed using a HORIBA LabRAM system equipped with a 50-mW 514-nm green laser. X-ray photoelectron spectroscopy (XPS) characterization was carried out using a Kratos AXIS ULTRA XPS system equipped with an Al Kα monochromatic X-ray source and a 165-mm mean radius electron energy hemispherical analyzer. X-ray diffraction (XRD) spectra were measured with a Bruker APEX system. Cross-sectional transmission electron microscopy (TEM) image was obtained by an FEI/Philips CM20 system, and plan-view TEM image was acquired by an FEI Tecnai12 system. Atomic force microscopy (AFM) characterization was performed using a Veeco Dimension 5000 system. Some characterizations were done on transferred graphene films, which were removed from Fe substrates by etching of substrate in $FeCl_3$ solution and the assistance of a polymethyl methacrylate (PMMA) coating layer [16].

3. Results and discussion

Fig. 1 shows a set of optical microscopy images of as-grown graphene samples on Fe substrates at growth temperatures between 250 °C and 800 °C with a step of 50 °C. Significant change in morphology of graphene films is observed. At low growth temperatures (≤350 °C), no film is visible. Starting from 400 °C, graphene flakes are formed and enlarged with the increase of the growth temperature. Graphene film extends to cover the whole substrate as the growth temperature reaches 550 °C. From 600 °C, graphene films can still be seen, however, condensed graphene domains start to appear randomly. The domains become larger and thicker with the increase of growth temperature. It should be noted that micrometer-sized graphene flakes are grown at a growth temperature as low as 400 °C, and large-area continuous graphene films on Fe are achieved at growth temperature of 500–550 °C, while much higher growth temperature is required to form graphene on other metal substrates (Cu, Co, etc.) [5–12].

Fig. 2(a) shows a typical Raman spectrum of graphene grown on Fe at 550 °C, in which the G (1594 cm^{-1})/2D (2709 cm^{-1}) ratio is 1.1, indicating that the as-grown film is few-layer graphene. D peak located at 1350 cm^{-1} is also seen in the spectrum, indicating that defects exist in the graphene film grown at 550 °C [17]. The inset shows a Raman mapping image of graphene grown at 550 °C. Over 80 points were measured over a mapping area of 40 μm × 40 μm. Mapping was done with respect to the intensity of the G peak, which provides graphene thickness information. As seen from the image, graphene signal is observed across all the area. In addition, most area is uniform in thickness (green color), while some area is thicker (red color). It is consistent with the optical microscope imaging results, namely, the as-grown graphene is locally uniform with darker spots representing thicker film (Fig. 1g).

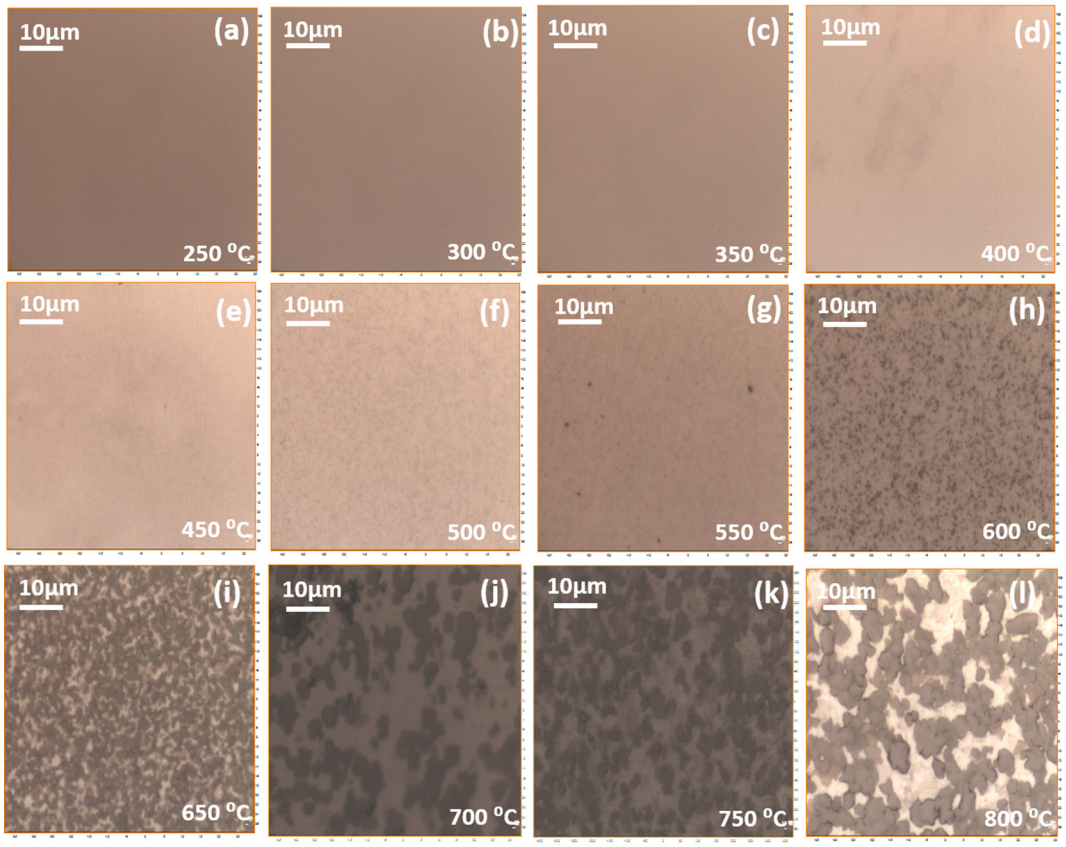

Fig. 1. (a)–(l) Optical microscopy images of graphene samples grown on Fe at different substrate temperatures. As temperature is below 350 °C, there is no obvious growth. Graphene flakes are seen at 400 °C, and keep enlarging with the increase of temperature. As temperature is between 500 °C and 550 °C, the Fe substrates are fully covered by uniform graphene films. As temperature is over 600 °C, condensed graphite grains are observed.

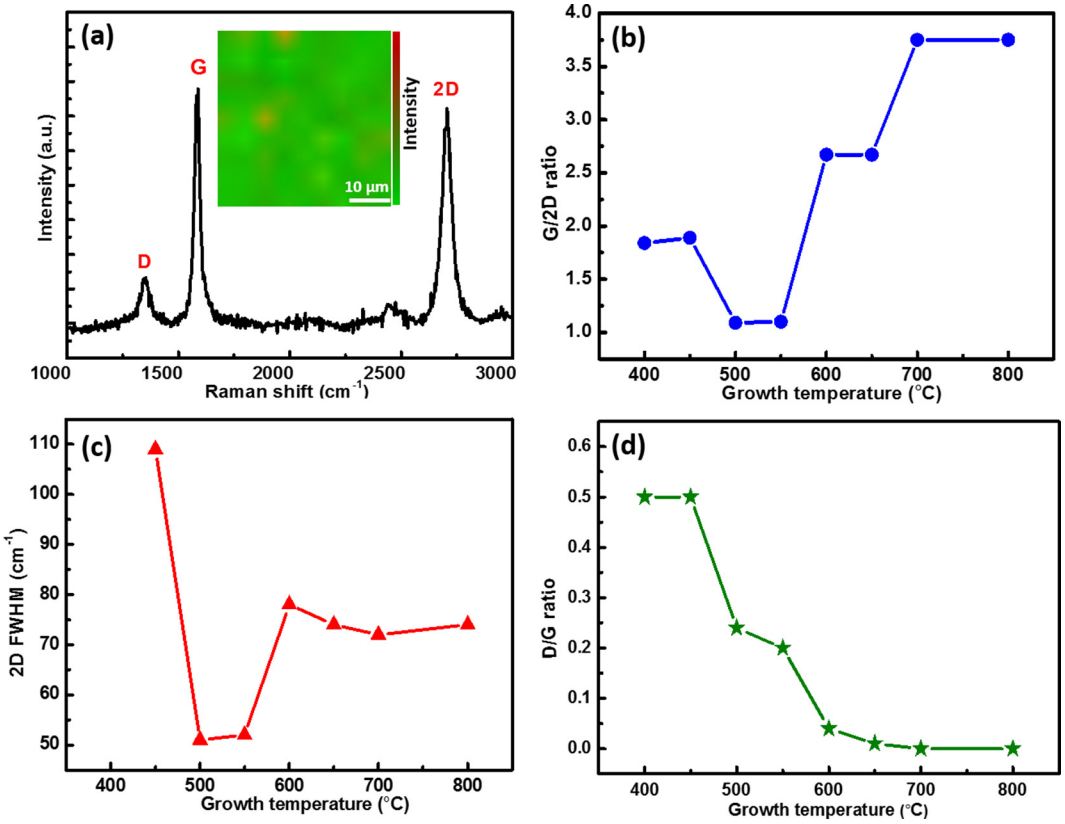

Fig. 2. Raman analysis of graphene samples grown on Fe at different temperature. (a) A typical Raman spectrum of a sample grown at 550 °C. G/2D ratio indicates that it is few-layer graphene. D peak is also evident. The inset is a Raman mapping result of graphene film grown at 550 °C. The mapping area is 40 μm × 40 μm. (b) G/2D ratio, (c) FWHM of 2D peak, (d) and D/G ratio as a function of growth temperature for samples grown from 400 °C to 800 °C.

Fig. 2(b) shows G/2D ratio and Fig. 2(c) shows full width at half maximum (FWHM) of 2D peaks from Raman spectra of the samples grown from 400 °C to 800 °C, respectively. The lowest G/2D ratio is ~1 as the growth temperature is between 500 °C and 550 °C. Similar trend is shown in measured FWHM, which reaches its minimum of ~50 cm^{-1} at the same growth temperature range, indicating again that the graphene film has 2 or a few layers [18]. Fig. 2(d) shows D/G ratio as a function of growth temperature, which reflects relative density of defects in the graphene films [19]. As seen from Fig. 2(d), D peak is always detected as growth temperature is lower than 650 °C, and disappears as the temperature exceeds 700 °C. Similar results of temperature-dependent effect on D peak were also observed for graphene grown on other metals [20–22].

Fig. 3 shows XRD patterns of graphene samples grown at different temperatures. Fe [110], [200] and [211] peaks are evident in the spectra of all these samples, showing that Fe thin films are polycrystalline [23, 24]. Graphitic signal, which is located at 27.5 2θ diffraction angle [25], is observed for the samples grown at a temperature of 600 °C and higher. The intensity of the graphene peak increases with the increase of temperature. This result is in close agreement with optical microscopy result shown in Fig. 1: As the temperature is higher than 600 °C, graphite features form instead of graphene films. 2θ diffraction peaks at 38.2° and 43° are observed for the samples grown between 350 °C and 650 °C, which indicates the existence of various iron carbide Fe_xC_y with different Fe and C mole fractions, including cementite (Fe_3C) [26]. As the temperature is lower than 350 °C, C solubility in Fe is so low that Fe_xC_y cannot be formed. As the temperature is higher than 650 °C, decomposition of Fe_xC_y into Fe and graphite speeds up, which essentially prevents the formation of graphene thin film. Only within a growth temperature window, in this case, 350–650 °C, the formation and decomposition of Fe_xC_y can be balanced to form graphene films. It suggests that the graphene on Fe growth is not a simple layer-by-layer deposition process or C precipitation process, but related to the chemical reaction of C and Fe atoms.

Fig. 4 shows XPS spectrum of the graphene sample grown at 550 °C. Graphene-like C sp^2 peak is located at 284.8 eV, and C-O peak (288.3 eV) is also observed [27]. In addition, Fe 2p 3/2 and 2p 1/2 peaks are detected [28]. With these different phases of Fe, high-quality graphene film can still form on Fe, further indicating that the chemical reaction of C and Fe has played an important role in the formation of graphene.

Fig. 5(a) shows a low-magnification cross-sectional TEM image of the graphene sample grown at 550 °C. The surface of Fe thin film is

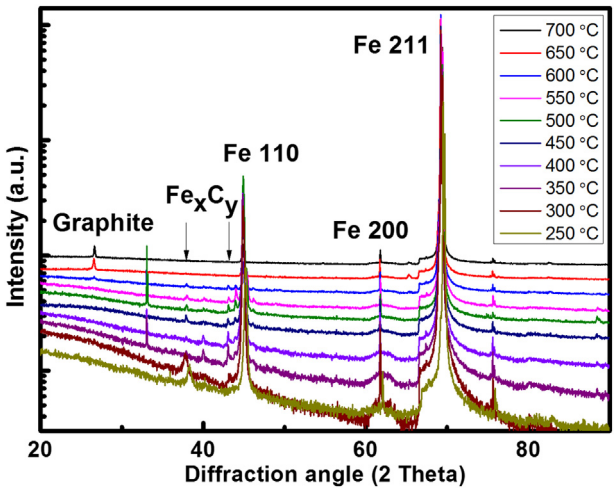

Fig. 3. XRD patterns of graphene samples grown on Fe at different temperatures. Graphite signal is detected as growth temperature is higher than 600 °C. Fe_xC_y signal is observed as the growth temperature is between 350 °C and 600 °C.

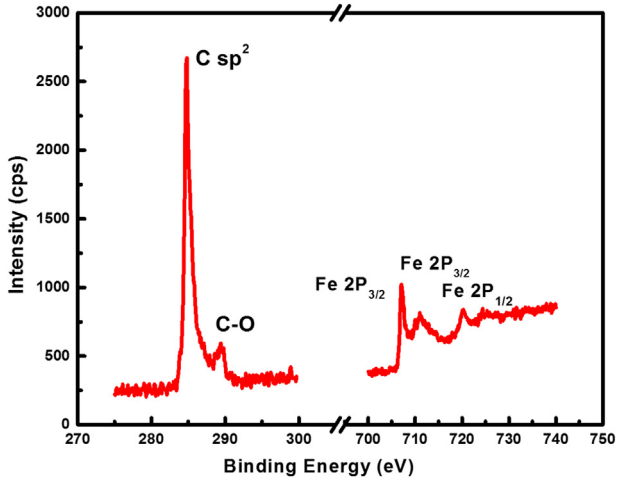

Fig. 4. XPS spectrum of graphene sample grown on Fe at 550 °C. C sp^2, C-O peak, Fe 2p 3/2, and Fe 2p 1/2 peaks are detected.

not flat, which is originated from the heat treatment at the growth temperature. It is evident that a continuous graphene film grows conformally on the Fe substrate. Nevertheless, the film thickness is not uniform across the surface. The inset of Fig. 5(a) shows a high-magnification view of a thicker film area. Layered graphene with a measured inter-layer distance of 0.34 nm is evident, which matches out-of-plane inter-layer distance of graphene very well. Fig. 5(b) shows a plan-view TEM image of the sample grown at 550 °C. Relatively thin and uniform graphene film with some darker spots representing thicker areas is observed. The inset shows a clear selected area electron diffraction (SAED) pattern, leading to a calculated A-plane distance of 0.211 nm, which is in good agreement with the theoretical value of graphene. Fig. 5(c) shows an AFM image of a transferred graphene on SiO_2. Most areas are flat and thin. A line scan profile shown in the inset reveals a thickness of about 0.7 nm, which indicates the existence of a bi-layer graphene. This result is in close agreement with the Raman result of this sample shown earlier. Some bright spots observed in the AFM image could be either related to the convex areas in the graphene film, which are inherited from rough Fe surface, or from thicker graphene domains.

Finally we briefly discuss the graphene growth mechanism. As the temperature is lower than 350 °C, the solubility of C in Fe is low, therefore, reaction between C and Fe is negligible, leading to no graphene growth. As the temperature is higher than 350 °C, enough C atoms are dissolved into Fe substrate and react with Fe to form iron carbide: Fe + C → Fe_xC_y, which transform into graphene at the same time: Fe_xC_y → Fe + C. The sequential reaction and decomposition mechanism leads to the growth of graphene in the intermediate temperatures (400–650 °C). As the temperature is higher than 650 °C, the formation and decomposition speed of Fe_xC_y increases drastically, which leads to the quick formation of discrete thick graphite domains rather than 2-D uniform graphene films. Thus, the formation and decomposition of Fe_xC_y plays an indispensable role in the growth of graphene on Fe, which is different with graphene growth on other metals.

4. Conclusion

We have carried out temperature-dependent growth of graphene thin films on Fe by MBE. Graphene begins to grow at a very low temperature of 400 °C and covers entire Fe surface at a relatively low temperature of 500–550 °C. Graphitic islands dominate the growth at a temperature higher than 600 °C. It is found that the formation/decomposition of Fe_xC_y is responsible for the growth of graphene on Fe, which differs with the precipitation growth of graphene on some other metals.

Acknowledgement

This work was supported by FAME, one of six centers of STARnet, a Semiconductor Research Corporation program supported by MACRO and DARPA.

References

[1] K.S. Novoselov, A.K. Geim, S.V. Morozov, D. Jiang, Y. Zhang, S.V. Dubonos, I.V. Grigorieva, A.A. Firsov, Electric field effect in atomically thin carbon films, Science 306 (2004) 666–669.
[2] K.V. Emtsev, A. Bostwick, K. Horn, J. Jobst, G.L. Kellogg, L. Ley, J.L. McChesney, T. Ohta, S.A. Reshanov, J. Röhrl, E. Rotenberg, A.K. Schmid, D. Waldmann, H.B. Weber, T. Seyller, Towards wafer-size graphene layers by atmospheric pressure graphitization of silicon carbide, Nat. Mater. 8 (2009) 203–207.
[3] M. Hajlaoui, H. Sediri, D. Pierucci, H. Henck, T. Phuphachong, M.G. Silly, L. De Vaulchier, F. Sirotti, Y. Guldner, R. Belkhou, A. Ouerghi, High electron mobility in epitaxial trilayer graphene on off-axis SiC (0001), Scientific Reports 6, 2016.
[4] C. Faugeras, A. Nerrière, M. Potemski, A. Mahmood, E. Dujardin, C. Berger, W.A. de Heer, Few-layer graphene on SiC, pyrolitic graphite, and graphene: a Raman scattering study, Appl. Phys. Lett. 92 (2008) 011914.
[5] Z.J. Wang, G. Weinberg, Q. Zhang, T. Lunkenbein, A. Klein-Hoffmann, M. Kurnatowska, M. Plodinec, Q. Li, L. Chi, R. Schloegl, M.G. Willinger, Direct observation of graphene growth and associated copper substrate dynamics by in situ scanning electron microscopy, ACS Nano 9 (2015) 1506–1519.
[6] K.S. Kim, Y. Zhao, H. Jang, S.Y. Lee, J.M. Kim, K.S. Kim, J.H. Ahn, P. Kim, J.Y. Choi, B.H. Hong, Large-scale pattern growth of graphene films for stretchable transparent electrodes, Nature 457 (2009) 706–710.
[7] L.L. Patera, C. Africh, R.S. Weatherup, R. Blume, S. Bhardwaj, C. Castellarin-Cudia, A. Knop-Gericke, R. Schloegl, G. Comelli, S. Hofmann, C. Cepek, In situ observations of the atomistic mechanisms of Ni catalyzed low temperature graphene growth, ACS Nano 7 (9) (2013) 7901–7912.

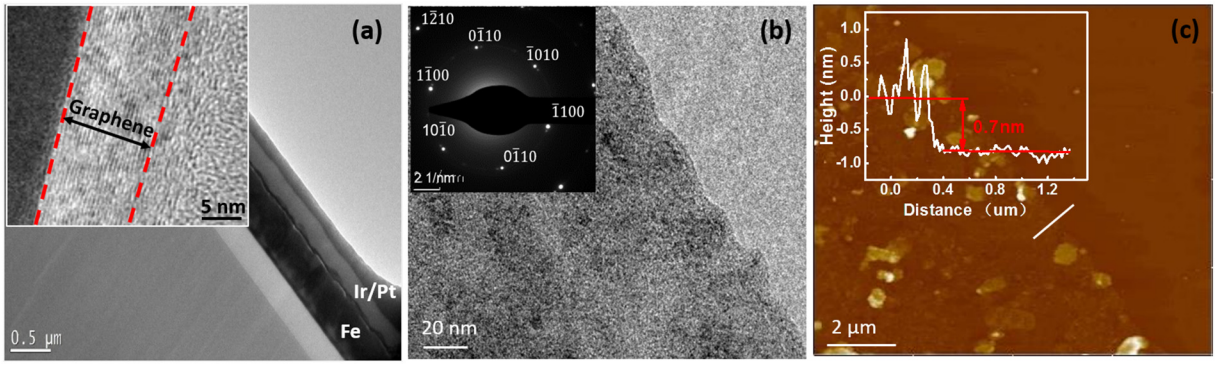

Fig. 5. (a) Cross-sectional TEM image of graphene sample grown on Fe at 550 °C. Graphene is seen in between Fe substrate and Ir/Pt protection layers used during TEM sample preparation. The inset is a higher-magnification TEM image of a local thicker film region on this sample, showing graphene layered structure. (b) Plan-view TEM image of a transferred graphene film from the sample grown at 550 °C. The inset is its SAED pattern. (c) AFM image of a transferred graphene film on SiO_2. The inset shows a line scan profile, indicating a graphene thickness of about 0.7 nm.

[8] N. Zhan, G.P. Wang, J.L. Liu, Cobalt-assisted large-area epitaxial graphene growth in thermal cracker enhanced gas source molecular beam epitaxy, Appl. Phys. A Mater. Sci. Process. 105 (2011) 341.
[9] I. Hernández-Rodríguez, J.M. García, J.A. Martín-Gago, P.L. de Andrés, J. Méndez, Graphene growth on Pt (111) and Au (111) using a MBE carbon solid-source, Diam. Relat. Mater. 57 (2015) 58–62.
[10] P. Sutter, J.T. Sadowski, E. Sutter, Graphene on Pt (111): growth and substrate interaction, Phys. Rev. B 80 (2009) 245411.
[11] R.S. Weatherup, A.J. Shahani, Z.J. Wang, K. Mingard, A.J. Pollard, M.G. Willinger, R. Schloegl, P.W. Voorhees, S. Hofmann, In situ graphene growth dynamics on polycrystalline catalyst foils, Nano Lett. 16 (2016) 6196–6206.
[12] P. Wu, W. Zhang, Z. Li, J. Yang, Mechanisms of graphene growth on metal surfaces: theoretical perspectives, Small 10 (2014) 2136–2150.
[13] N.A. Vinogradov, A.A. Zakharov, V. Kocevski, J. Rusz, K.A. Simonov, O. Eriksson, A. Mikkelsen, E. Lundgren, A.S. Vinogradov, N. Mårtensson, A.B. Preobrajenski, Formation and structure of graphene waves on Fe (110), Phys. Rev. Lett. 109 (2012) 026101.
[14] D. Kondo, S. Sato, K. Yagi, N. Harada, M. Sato, M. Nihei, N. Yokoyama, Low-temperature synthesis of graphene and fabrication of top-gated field effect transistors without using transfer processes, Appl. Phys. Express 3 (2010) 025102.
[15] D. Kondo, K. Yagi, M. Sato, M. Nihei, Y. Awano, S. Sato, N. Yokoyama, Selective synthesis of carbon nanotubes and multi-layer graphene by controlling catalyst thickness, Chem. Phys. Lett. 514 (2011) 294–300.
[16] W. Regan, N. Alem, B. Alemán, B. Geng, Ç. Girit, L. Maserati, F. Wang, M. Crommie, A. Zettl, A direct transfer of layer-area graphene, Appl. Phys. Lett. 96 (2010) 113102.
[17] M.M. Lucchese, F. Stavale, E.H.M. Ferreira, C. Vilani, M.V.O. Moutinho, R.B. Capaz, C.A. Achete, A. Jorio, Quantifying ion-induced defects and Raman relaxation length in graphene, Carbon 48 (2010) 1592–1597.
[18] Q.Q. Li, X. Zhang, W.P. Han, Y. Lu, W. Shi, J.B. Wu, P.H. Tan, Raman spectroscopy at the edges of multilayer graphene, Carbon 85 (2015) 221–224.
[19] C. Mattevi, G. Eda, S. Agnoli, S. Miller, K.A. Mkhoyan, O. Celik, M. Chhowalla, Evolution of electrical, chemical, and structural properties of transparent and conducting chemically derived graphene thin films, Adv. Funct. Mater. 19 (2009) 2577–2583.
[20] S.J. Chae, F. Güneş, K.K. Kim, E.S. Kim, G.H. Han, S.M. Kim, C.W. Yang, Synthesis of large-area graphene layers on poly-nickel substrate by chemical vapor deposition: wrinkle formation, Adv. Mater. 21 (2009) 2328–2333.
[21] F. Banhart, J. Kotakoski, A.V. Krasheninnikov, Structural defects in graphene, ACS Nano 5 (2010) 26–41.
[22] J.M. Wofford, S. Nie, K.F. McCarty, N.C. Bartelt, O.D. Dubon, Graphene islands on Cu foils: the interplay between shape, orientation, and defects, Nano Lett. 10 (2010) 4890–4896.
[23] J. WooáLee, S. BináKim, Enhanced Cr (VI) removal using iron nanoparticle decorated graphene, Nanoscale 3 (2011) 3583–3585.
[24] N.R. Tao, Z.B. Wang, W.P. Tong, M.L. Sui, J. Lu, K. Lu, An investigation of surface nanocrystallization mechanism in Fe induced by surface mechanical attrition treatment, Acta Mater. 50 (2002) 4603–4616.
[25] D. Geng, S. Yang, Y. Zhang, J. Yang, J. Liu, R. Li, S. Knights, Nitrogen doping effects on the structure of graphene, Appl. Surf. Sci. 257 (2011) 9193–9198.
[26] Y. Hu, J.O. Jensen, W. Zhang, L.N. Cleemann, W. Xing, N.J. Bjerrum, Q. Li, Hollow spheres of iron carbide nanoparticles encased in graphitic layers as oxygen reduction catalysts, Angew. Chem. Int. Ed. 53 (2014) 3675–3679.
[27] B. Wang, X.L. Wu, C.Y. Shu, Y.G. Guo, C.R. Wang, Synthesis of CuO/graphene nanocomposite as a high-performance anode material for lithium-ion batteries, J. Mater. Chem. 20 (2010) 10661.
[28] T. Yamashita, P. Hayes, Analysis of XPS spectra of Fe2 + and Fe3 + ions oxide materials, Appl. Surf. Sci. 254 (2008) 2441–2449.